Bioconjugate Chemistry

Article

pubs.acs.org/bc

Codendrimer from Polyamidoamine (PAMAM) and Oligoethylene Dendron as a Thermosensitive Drug Carrier

Yifei Guo,[†] Yanna Zhao,[†] Jing Zhao,[†] Meihua Han,[†] Afang Zhang,*[,‡] and Xiangtao Wang*[,†]

[†]Institute of Medicinal Plant Development, Chinese Academy of Medical Sciences, Peking Union Medical College, 151 Malianwa North Road, Beijing 100193, P. R. China

[‡]Department of Polymer Materials, College of Materials Science and Engineering, Shanghai University, Nanchen Street 333, Shanghai 200444, P. R. China

Supporting Information

ABSTRACT: The efficient synthesis of codendrimer PAMAM-co-OEG (**PAG**) and its properties in aqueous solution, including particle size and thermosensitivity, are described. **PAG** is synthesized with well-defined structure through the "attach to" route. In the aqueous solutions, **PAG** forms unimer and multimolecular aggregates with the respective particle sizes of approximately 8 and 200 nm, depending on the concentration. **PAG** shows thermosensitive behavior with sharp and fast transition, and the lower critical solution temperature is 38.2 °C. The suitability of codendrimer **PAG** as the thermosensitive carrier is evaluated with methotrexate (MTX) as the model drug. MTX is encapsulated in **PAG** with the drug-loading capacity of 39%, among which 30% of MTX is encapsulated in PAMAM core. The release behavior of MTX mediated by temperature is investigated with focus on the effects around the LCST of **PAG**.

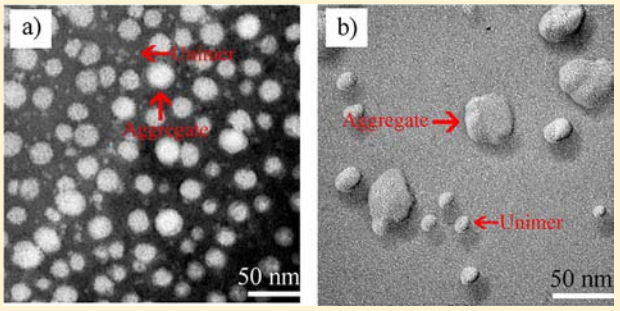

INTRODUCTION

Current approaches to cancer therapy rely on chemotherapeutic agents. Unfortunately, the poor solubility and side effects of these agents pose a great challenge for their possible applications in formulation development and clinical treatment. Recently, the development of drug delivery technologies has focused on polymeric unimolecular micelles formed by dendrimer or amphiphilic dendrimer-like copolymers, with which the advantages have been demonstrated.[1−3] Several studies have compared dendritic carriers to conventional polymeric micelles formed by linear amphiphilic copolymers, and proved that branched copolymer−drug conjugates are more active.[4,5] Besides, cellular uptake of dendrimer-based drug carriers were proven to be significantly higher than linear polymeric carriers.[6] These results demonstrate the unique potential of dendrimer architectures as drug carriers, and a number of such polymer systems have been developed in the past and been reviewed in several excellent articles.[7−10]

Among those dendrimers employed,[11,12] polyamidoamine (PAMAM) dendrimers, owing to their unique characteristics such as nanoscopic size range, low polydispersity, and predictable surface charge, stand out as superior drug carriers. However, their cytotoxicity inhibits their broad applications,[13,14] which leads to further structure modifications for their biorelated applications. Normally, PAMAMs are modified by conjugating with linear polyethylene glycol (PEG) chains,[15,16] PCL-PEG chains,[17] peptides,[18] anticancer drug,[19] targeting compounds,[20] cyclodextrins,[21] and amino acids.[22] Among these modifications, PEGs are used broadly due to their excellent water solubility, biocompatibility, and FDA approval for intravenous usage.

Despite many attempts having been made to utilize dendrimers or modified dendrimers for drug delivery, the applications in the biomedical field are expected to increase the delivery efficiency to the target site. Based on increasing therapeutic effects of the drug delivery system and the observation that the enhanced cellular uptake of thermosensitive polymers is observed at higher temperature associated with tumor tissues,[23] the modified dendrimers with thermosensitive properties have been extensively investigated.[24] In general, these thermosensitive dendrimers are prepared by modifying the outer dendrimer surface with thermosensitive polymers, during which, PAMAM, PPI, and Bolton H40 are used as the dendritic core, and PNIPAM, PDMA, DMA, and POEG are used as the thermosensitive shell.[3,25,26] However, dendrimers obtained using this approach might be regarded more as star polymers and might lose their important features such as highly defined structure and globular shape. To overcome these drawbacks, Kono's group incorporated various alkylamide groups, such as isobutyramide (IBAm) groups, to chain terminals of PAMAM dendrimers and poly(propyleneimine) dendrimers; these alkylamide-terminated dendrimers present

Received: October 12, 2012
Revised: October 18, 2013
Published: December 2, 2013

thermosensitive property and retain structural features of dendrimers.[27,28] And then, to enhance the biocompatibility of thermosensitive dendrimer, Kono and co-workers demonstrate that attachment of oxyethylene units to PAMAM dendrimer to provide both high temperature sensitivity and non-cytotoxic properties.[29] Recently, we have found that polymers carrying dendritic oligo(ethylene glycol) (OEG) side chains show attractive thermosensitive behavior; their lower critical solution temperature (LCST) can be tuned from 33 to 64 °C by the modification of the terminal groups, length of the OEG chains, or dendron generations. The thermosensitive OEG dendrons are nontoxic and have many advantages compared with the linear PEG counterparts; therefore, thermosensitive dendrimers conjugated with OEG dendrons could be expected to achieve both higher delivery efficiency and cellular uptake to the tumor tissues.[30−32]

Considering that thermosensitive properties are important for dendrimers to increase their efficiency as drug carries, we design in this paper a novel thermosensitive drug codendrimer PAMAM-co-OEG (**PAG**) by decorated fourth-generation PAMAM (**P4**) with the second-generation OEG dendron (G2). **PAG** is synthesized via the "attach-to" route to decorate the periphery completely, and its structure is characterized by ^{1}H NMR spectroscopy, GPC, and the UV labeling technique (Sanger's reagent). **PAG** undergoes sharp phase transitions at its LCST, thus making it more applicable for cancer therapy. A typical anticancer drug methotrexate (MTX), widely used for the treatment of certain human cancers, is selected as the model drug to evaluate codendrimer **PAG** as the thermosensitive drug carrier.

EXPERIMENTAL SECTION

Materials. Tosylated triethylene glycol monoethyl ether (Et-TEG-Ts) and compound **1** were synthesized according to previous reports.[30−32] Tetrahydrofuran (THF) was refluxed over lithium aluminum hydride (LAH), and dichloromethane (DCM) was distilled from CaH_2 for drying. Fourth-generation PAMAM (**P4**) and other reagents and solvents were purchased and used without further purification.

Synthesis of Compound 2. $LiOH{\cdot}H_2O$ (0.10 g, 1.64 mmol) was added into a solution of compound **1** (2.00 g, 0.82 mmol) in methanol (20 mL) and water (10 mL) at −5 °C with stirring, and the reaction temperature was allowed to increase to room temperature. After stirring for 3 h, the solvents were evaporated in vacuo at room temperature. The residue was dissolved with DCM, and the solution pH was adjusted carefully with 10% $KHSO_4$ aqueous solution to approximately 5−6. After the organic phase had been washed with brine and dried over $MgSO_4$, the crude product was purified by column chromatography with DCM/MeOH (20/1, v/v) to yield compound **2** as a slight yellow oil (1.90 g, 95%). ^{1}H NMR ($CDCl_3$): δ = 1.17−1.23 (t, 27H, CH_3), 3.48−3.50 (m, 18H, CH_2), 3.55−3.67 (m, 72H, CH_2), 3.70−3.74 (m, 18H, CH_2), 3.82−3.86 (m, 30H, CH_2), 4.12−4.16 (m, 18H, CH_2), 4.18−4.26 (m, 6H, CH_2), 4.46−4.48 (s, 6H, CH_2), 6.56−6.58 (s, 6H, CH), 7.45 (s, 2H, CH). ^{13}C NMR ($CDCl_3$): δ = 15.10, 66.55, 68.82, 69.05, 69.30, 69.57, 69.71, 69.77, 70.35, 70.47, 70.54, 70.63, 70.65, 70.77, 72.25, 72.48, 73.19, 106.23, 109.38, 125.26, 133.69, 137.86, 144.38, 152.59, 167.07.

Synthesis of Compound 3. The acid compound **2** (1.90 g, 0.78 mmol) and pentafluorophenol (0.22 g, 1.20 mmol) were dissolved in DCM (30 mL) and stirred for 10 min. DCC (0.37 g, 1.80 mmol) was then added. The mixture was stirred overnight at room temperature before washing with saturated $NaHCO_3$ and brine successively. After drying over $MgSO_4$, the organic phase was purified by column chromatography with DCM/MeOH (40/1, v/v) to yield a slightly yellow oil (1.50 g, 74%). ^{1}H NMR ($CDCl_3$): δ = 1.19−1.24 (t, 27H, CH_3), 3.38−3.46 (m, 18H, CH_2), 3.50−3.63 (m, 72H, CH_2), 3.68−3.74 (m, 18H, CH_2), 3.80−3.86 (m, 30H, CH_2), 4.10−4.15 (m, 18H, CH_2), 4.23−4.29 (m, 6H, CH_2), 4.58−4.62 (s, 6H, CH_2), 6.40−6.42 (s, 6H, CH), 7.40 (s, 2H, CH). ^{13}C NMR ($CDCl_3$): δ = 15.10, 61.70, 66.55, 68.82, 69.05, 69.30, 69.57, 69.71, 69.77, 70.35, 70.47, 70.54, 70.63, 70.65, 70.77, 72.25, 72.48, 73.19, 107.23, 110.38, 121.26, 133.69, 137.86, 144.38, 152.59, 162.07.

Synthesis of Codendrimer PAG. The solution of compound **3** (1.12 g, 0.43 mmol) in DMF (20 mL) was added into a solution of **P4** (64 mg, 4.50 μmol), TEA (27 mg, 0.27 mmol), and DMAP (20 mg) in mixed solvent DMF/H_2O (50 mL, 1/1, v/v) at −5 °C with stirring, and the reaction temperature was allowed to increase to room temperature. After stirring for 48 h, the solvents were evaporated in vacuo at room temperature. The residue was dissolved with H_2O and purified by dialysis (MWCO 3500) against MeOH (6 × 1 L), which yielded **PAG** as a colorless oil (0.56 g, 70%). ^{1}H NMR (DMSO-d_6): δ = 1.10 (br, CH_3), 3.28−3.65 (br, CH_2), 3.65−3.80 (br, CH_2), 4.17−4.28 (br, CH_2), 4.38−4.50 (br, CH_2), 6.50−6.70 (br, CH). ^{13}C NMR (DMSO-d_6): δ = 14.65, 38.87, 39.14, 39.42, 39.70, 39.78, 40.26, 65.24, 68.60, 68.96, 69.66, 69.71, 69.74, 69.84, 71.67, 71.82, 107.08, 133.66, 137.42, 151.94. Elemental analysis (%) calcd for $C_{8174}H_{14176}N_{250}O_{3260}$, 168033.16: C, 58.37%; H, 8.52%; N, 2.08%; O, 31.02%. Found: C, 57.73%; H, 8.37%; N, 2.37%; O, 31.05.

Quantification of Dendronization. A well-stirred solution of codendrimer **PAG** (15 mg) in 1,1,2,2-tetrachloroethane (0.5 mL) was treated with 0.1 M $NaHCO_3$ solution (0.1 mL), and a solution of Sanger's reagent (0.3 equiv per amine groups) in 1,1,2,2-tetrachloroethane (0.5 mL) was added. The reaction mixture was stirred at 65 °C for 3 h and then cooled to room temperature. 1,1,2,2-Tetrachloroethane (2 mL) and water (2 mL) were added to the mixture. The organic layer was separated, washed with water (1 mL) and brine (1 mL) and concentrated in vacuo. The residue was purified by column chromatography with DCM to yield a yellow solid, the 2,4-dinitrophenyl-labeled dendrimers (13 mg, 87%).

Critical Aggregation Concentration (CAC). The **CAC** of codendrimer was estimated by a fluorescence spectroscopic method using pyrene (Py) as the probe. Typically, Py solutions in acetone were added to each EP tube. The acetone was then evaporated, leaving 6.0 × 10^{-5} mol of Py in each tube. Aqueous **PAG** solutions with various concentrations (from 1.0 × 10^{-4} to 2.5 mg/mL) were prepared and added to the tubes. The mixtures were sonicated for 2 min and stirred at room temperature for 12 h. The spectroscopy measurements were conducted at an emission wavelength of 372 nm and an excitation wavelength of 334 nm.

Hemolytic Effect. About 5 mL of blood from a male New Zealand white rabbit was drawn from the ear artery. The red blood cell (RBC, 2% w/v) solution was prepared and centrifuged at 3000 rpm for 5 min. The plasma supernatant was removed, and the erythrocytes were resuspended in normal saline solution. The cells were again centrifuged at 3000 rpm for 5 min. The micellar formulations were incubated with the 2% (w/v) RBC suspension at 37 °C for a predetermined time with different codendrimer concentrations. The RBCs were removed by centrifugation, 100 μL of the supernatant was

dx.doi.org/10.1021/bc300560p | Bioconjugate Chem. 2014, 25, 24−31

Scheme 1. Synthesis of the Codendrimer PAG[a]

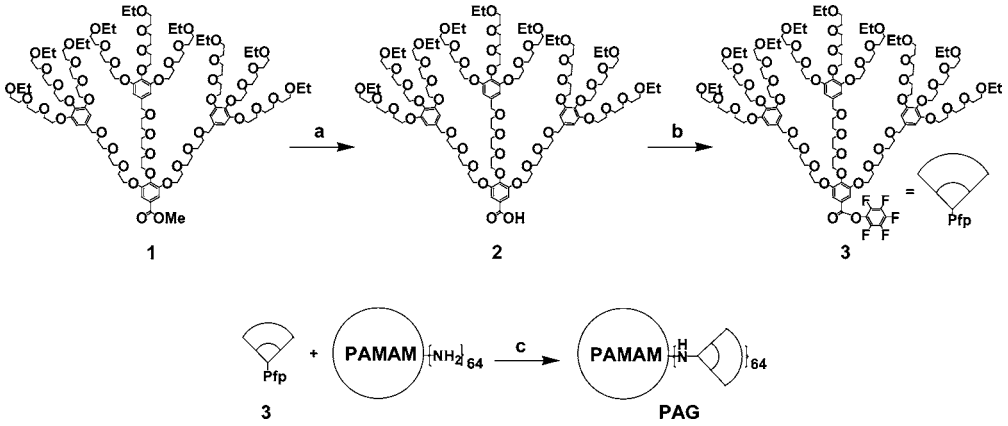

[a]Reagents and conditions: (a) LiOH, MeOH, −5 to 25 °C, 3 h (95%); (b) Pfp, DCC, DCM, 25 °C, 12 h (74%); (c) **P4**, TEA, DMAP, DMF, −5 to 25 °C, 24 h (70%). Pfp = pentafluorophenol, DCC = dicyclohexylcarbodiimide, DCM = dichloromethane, TEA = triethylamine, DMAP = *N,N*-dimethylaminopyridine, DMF = dimethylformamide.

pipetted into a 96-microwell plate, and the absorbance was measured at 540 nm using a microplate reader (Versamax Tunable Microplate Reader). The results were expressed as percentage hemolysis with the assumption that deionized water causes 100% hemolysis and NS solution 0% hemolysis. The experiments were conducted in triplicate, and the data were shown as the mean values plus standard deviation (±SD). All experimental procedures were performed in accordance with the Guidelines for Ethical and Regulatory for Animal Experiments as defined by the Institutional Animal Care and Use Committee of Peking University Health Science Center.

Preparation of Drug-Loaded Micelles. Drug-loaded micelles were prepared by the dialysis method. Briefly, the codendrimer (2 mg) and methotrexate (MTX, 2 mg) were dissolved in DMF (1 mL) in a glass vial at room temperature. After that, the deionized water (5 mL) was added dropwise into this vial at 4 °C under vigorous stirring. The mixed solution was transferred into the dialysis bag (MWCO 14000) and dialyzed against 150 mM NaCl solution (4 L) for 4 h to remove the free MTX at room temperature and 42 °C separately. The entrapment efficiency (EE) and drug loading content (DL) were measured by UV−vis spectrophotometer and calculated as follows:

$$\mathrm{EE} = (\text{weight of loaded drug/weight in feed}) \times 100\%$$

$$\mathrm{DL} = (\text{weight of loaded drug/weight of drug} - \text{loaded codendrimer}) \times 100\%$$

In Vitro Drug Release. The MTX-loaded micelles solution (2 mL) was transferred into a dialysis bag (MWCO 14000). It was immersed in 50 mL of 150 mM NaCl solution. The release studies were performed at 37 and 42 °C, respectively, with continuous magnetic stirring at 100 rpm. At predetermined time intervals, 2 mL of the external solution was withdrawn and replenished with an equal volume of fresh media for analysis. The drug release study was performed for 98 h. The amount of MTX released was analyzed with a UV−vis spectrophotometer. The release experiments were conducted in triplicate. The data were shown as the mean values plus standard deviation (±SD).

Instrumentation and Measurements. ^{1}H NMR spectra were recorded on a Bruker AV 600 (600 MHz) spectrometer, and chemical shifts were reported as δ values (ppm) relative to internal Me_4Si. Gel permeation chromatography (GPC) measurements were carried out on a Viscotek GPC VE2001 instrument with single column set equipped with refractive index detector and DMF (containing 1 g/L LiBr) as the eluent at 35 °C. Calibration was performed with PMMA standards. UV/vis turbidity measurements were conducted on a PE UV−vis spectrometer (Lambda 35) equipped with a thermostatically regulated bath. Aqueous polymer solutions were placed in the spectrophotometer (path length 1 cm) and heated or cooled at a rate of 0.2 °C/min. The absorption of the solution at λ = 500 nm was recorded every 5 s. The LCST was determined to be the value at which the transmittance at λ = 500 nm reached 50% of its initial value. Dynamic light scattering measurements were performed on a Zetasizer Nano-ZS analyzer (Malvern Instruments) with an integrated 4 mV He-Ne laser, λ = 633 nm, which used backscattering detection (scattering angle θ = 173°) at room temperature and 50 °C, respectively. TEM and cryo-TEM studies were performed with a Hitachi H-7650 instrument at a voltage of 80 kV. Samples for TEM were prepared by drop-casting codendrimer solutions onto carbon-coated copper grids, air-drying them at room temperature, and then dyeing them with phosphotungstic acid. Fluorescent measurements were conducted on a F-4500 FL spectrophotometer, and the fluorescence emission spectra of pyrene (concentration 6 × 10^{-5} M) in the presence of various concentrations of **PAG** aqueous solution at 25 °C were recorded at an excitation wavelength of 334 nm.

RESULTS AND DISCUSSION

Synthesis. The synthesis procedures of **PAG** are shown in Scheme 1. Compounds **1**, **2**, and **3** were synthesized according to previous reports.[30−32] The second generation OEG dendron **1** was first hydrolyzed with lithium hydroxide in a mixed solvent of methanol and water to obtain the dendron acid **2** with a yield of 95%, which was then reacted with pentafluorophenol in the presence of dicyclohexylcarbodiimide (DCC) as the coupling reagent to afford the corresponding active esters **3** with a yield of 74%. These compounds were fully characterized by ^{1}H and ^{13}C NMR spectroscopy.

The codendrimer **PAG** was synthesized via the "attach-to" route by coupling the active ester **3** with the peripheral amino-groups of dendrimer **P4**.[33] After purification by dialysis against

dx.doi.org/10.1021/bc300560p | *Bioconjugate Chem.* 2014, 25, 24−31

MeOH (MWCO 3500), **PAG** was obtained with a yield of 70%. The results are summarized in Table 1. In contrast to

Table 1. Conditions for and Results from the Coupling of P4 and G2

				GPC results[a]		
entries	$[NH_2]$:[G2]	time (h)	yield (%)	Mn × 10^{-5}	PDI	LCST[b] (°C)
P4	-	-	-	0.14	1.01	n.d.[c]
PAG	1:3	48	70	1.97	1.00	38.2

[a]MeOH for **P4** and DMF (0.02 M LiBr) for **PAG** at 35 °C. [b]The apparent LCST of the polymer was determined as the temperature at which the transmittance was 50% of the initial transmittance. [c]Not detected.

PAMAM, which is soluble only in water, **PAG** is highly soluble in conventional solvents, such as dichloromethane, THF, MeOH, as well as water, due to the excellent solubility of the OEG shell. The ^{1}H NMR spectrum of **PAG** was recorded in DMSO-d_6 at 50 °C to achieve better resolution (Figure 1). Even so, most proton signals from the OEG moieties were broadened, and the signals from PAMAM moieties almost immersed under the baseline. The molar mass of **PAG** was determined by GPC with DMF as the eluent to be 1.97 × 10^5, and its PDI is 1.00.

Characterization. The coverage degree of **PAG** was first determined by ^{1}H NMR spectroscopy. For this purpose, the signal intensity of $-CH_3$ from the OEG dendron at δ = 1.00 was compared with that of $-CH_2CO$ from the PAMAM core at δ = 2.20, and the result was 9.08, which was higher than the theoretical value of 7.00 for a 100% coverage. The reason for this contradiction should come from the shielding effect of OEG dendrons. After covering the periphery of PAMAM densely with the OEG dendron, OEG dendron provided a shell which hindered the mobility of the inner core of PAMAM, thus may lead to difficulty for being detected by NMR spectroscopy. Second, the coverage degree of **PAG** was estimated by comparing the molar mass and PDI. According to GPC measurement (Figure 2), the molar mass of **PAG** was 1.97 × 10^5 and the PDI was 1.00. For **PAG** with 100% coverage, its

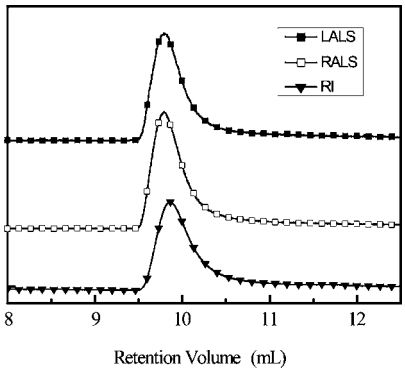

Figure 2. GPC traces for codendrimer **PAG**.

molar mass was calculated to be 1.68 × 10^5, which is similar to the measured one. The measured narrow PDI also indicated that **PAG** was synthesized successfully with higher grafting degree. Third, the structural fidelity of **PAG** was also investigated using a UV labeling technique, which was determined by treating the remaining nondendronized amine groups of **PAG** with 2,4-dinitrofluorobenzene (Sanger's reagent),[33] and the coverage degree of **PAG** was 99.8%. All these results indicated the PAMAM was decorated by the OEG dendron in excellent coverage.

Aggregation Properties. According to the structure of codendrimer **PAG**, it should be dissolved molecularly in water due to the excellent solubility enhancement by the peripheral OEG dendron. Dynamic light scattering was utilized to detect **PAG** sizes in aqueous solutions at different concentration (0.01, 0.1, 1.0, 10 mg/mL), and the results are shown in Figure 3a. It was obvious that the particle size and its distribution were dependent on the concentration of the codendrimer. At low concentration (0.01 mg/mL), single distribution with a small size component of approximately 8 nm was shown, which should correspond to the unimer of **PAG** presented in such a concentration. However, when the concentration was increased to 1.0 mg/mL, it demonstrated a bimodal distribution with a smaller-sized component of approximately 8 nm (95% in proportion) and a large-sized component of approximately 110 nm (5% in proportion), which confirmed that **PAG** partially

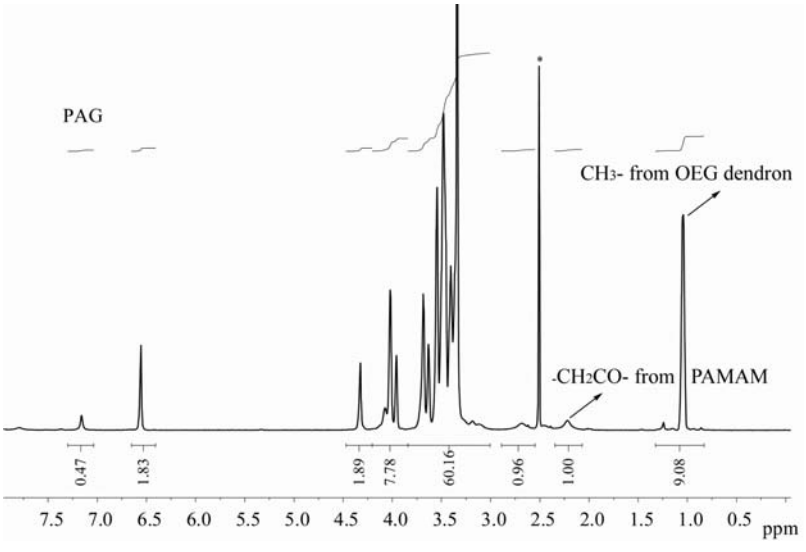

Figure 1. ^{1}H NMR spectrum of **PAG** in DMSO-d_6.

dx.doi.org/10.1021/bc300560p | *Bioconjugate Chem.* 2014, 25, 24−31

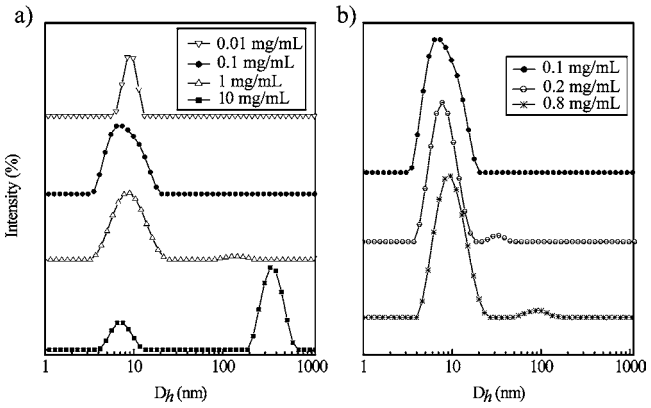

Figure 3. DLS graph of the size distribution of codendrimer **PAG** in aqueous solutions.

changed from unimer to aggregates. Further increasing concentration to 10 mg/mL, the bimodal distribution remained, but the proportion of large particle was increased from 5% to 70% and its size also increased from 110 to 200 nm. These results suggest that **PAG** presented in aqueous solutions with both unimer and aggregates, depending on the solution concentration. The secondary aggregation of unimolecular micelles to large polymeric micelles had been reported for similar amphiphilic dendritic systems.[17,34,35] To find its critical aggregation concentration (CAC), **PAG** with different concentrations were further recorded (Figure 3b). Based on these results, the apparent CAC of **PAG** in aqueous solutions was calculated to be 0.1 mg/mL.

The direct morphology analysis of **PAG** aggregates formed in aqueous solutions was conducted by transmission elctron microscopy (TEM) using negative staining and cryo-TEM measurements at a concentration of 0.2 mg/mL, and the micrographs are shown in Figure 4. Both the TEM and cryo-

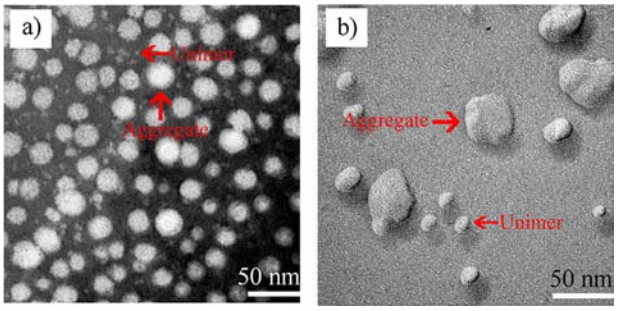

Figure 4. Micrograph of **PAG**: (a) TEM and (b) cryo-TEM.

TEM micrographs revealed the existence of two different forms for the codendrimer **PAG** in water: the unimers were spherical with a diameter of 6–8 nm, while the larger aggregates with diameter approximately of 30 nm should be formed by several unimers.

The aggregation behavior of codendrimer **PAG** was further characterized by fluorescence spectroscopy using pyrene as a probe, which was sensitive to the surrounding environment, and the ratio of the intensities of the third (384 nm) and first (372 nm) peaks (I_3/I_1) was used to confirm the CAC. To a saturated aqueous solution of pyrene, different concentrations of **PAG** were checked, and the evolution of I_3/I_1 as a function of **PAG** concentration is shown in Figure 5. It was shown that

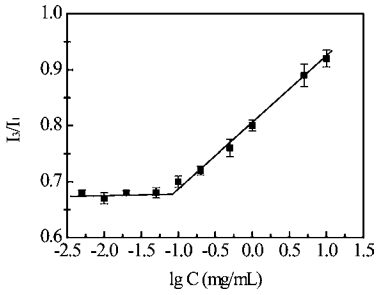

Figure 5. Dependence of intensity ratio I_3/I_1 as a function of codendrimer **PAG** concentration.

the ratio values of I_3/I_1 remained constant below the CAC and then changed substantially, and the CAC was detected as 0.1 mg/mL. The existence of a CAC for codendrimer **PAG** was consistent with previous observation in the DLS. Although **PAG** aggregates would be dissociated after injected in vivo, the unique chemical structure of **PAG** will be maintained, which would act as unimolecular micelles to encapsulate anticancer drug.

Thermosensitive Behavior. It has been well established that OEG-based polymers become dehydrated in aqueous solutions and undergo a phase transition from molecularly dissolved homogeneous solution to heterogeneous aggregates around their LCST. Similar to OEG-based polymers, **PAG** was water-soluble at room temperature, but showed thermosensitive behavior after heating up to its LCST. UV–vis spectrophotometry was thus applied to investigate the thermoresponsive behavior of **PAG** and to determine its apparent LCST. The turbidity curves measured from 34 to 42 °C are plotted in Figure 6a. The conclusions gained from these curves are as follows: (1) codendrimer **PAG** decorated by OEG dendron showed typical thermoresponsive behavior, and its LCST is 38.2 °C; (2) phase transitions are very sharp (≤0.3

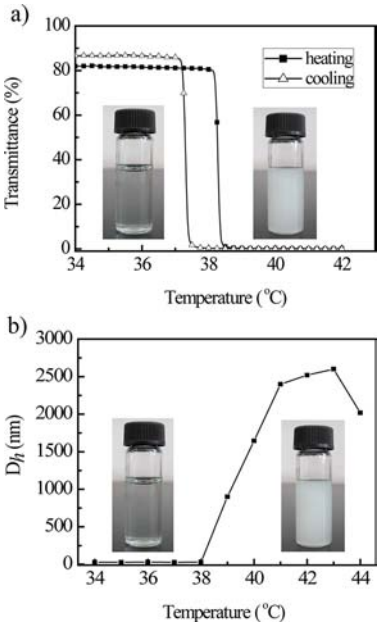

Figure 6. (a) Plots of the transmittance vs temperature for 0.5 wt % aqueous solutions of **PAG** with heating and cooling rates = 0.2 °C/min. (b) Plots of the hydrodynamic diameters (D_h) vs temperature for 0.5 wt % aqueous solutions of **PAG**.

dx.doi.org/10.1021/bc300560p | *Bioconjugate Chem.* 2014, 25, 24–31

°C) and hystereses (≤1 °C) between the heating and cooling processes are small, which was indicative of a very narrow PDI.[36] The thermally induced aggregation of the codendrimer was further investigated by DLS to record the temperature-dependent aggregate size, and the results are plotted in Figure 6b. The **PAG** solutions (5 mg/mL) were fully transparent at 35 °C; with increasing the temperature, the aggregate sizes showed a sharp transition and reached a large value resulting from intermolecular aggregation. Compared to the dendronized polymer and dendrimer from the same OEG dendron with LCSTs of 36 °C, **PAG** showed a slightly higher LCST, which was likely caused by the interior PAMAM. The LCST of **PAG** (38.2 °C) is slightly higher than normal tissue temperature (37 °C), which suggests that **PAG** can encapsulate the anticancer drug and remain stable during systemic circulation. Then, when they arrive at the tumor site with slight higher temperature, the OEG dendron shell changes from hydrophilic to hydrophobic which increases the cellular uptake due to the relatively hydrophobic character of the cell surface; the codendrimers with the hydrophobic character strongly interact with cells and could be taken up efficiently by the cells.[10,29,37,38] This property indicates that **PAG** is suitable as a thermosensitive drug carrier due to its aggregation at the tumor site induced by slight temperature difference.

Hemolytic Effect. The hemolytic effect of **PAG** on rabbit RBC was investigated to verify the suitability via intravenous administration (Figure 7). The hemolysis rate curves of **PAG**

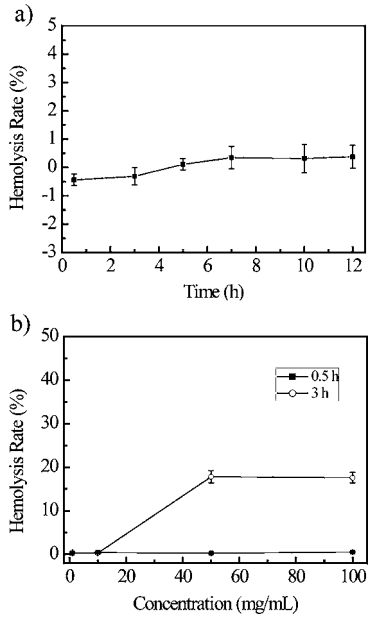

Figure 7. Hemolytic activity of **PAG** with a concentration of 10 mg/mL (a) and the concentration dependence (b).

with 10 mg/mL from 0.5 to 12 h are shown in Figure 7a, and no hemolytic activity (<0.5%) was found. The dependence of the hemolytic activity on the concentration of **PAG** was also investigated. Concentrations ranging from 1 to 100 mg/mL showed no hemolytic activity within 0.5 h, although prolonging the time to 3 h led to a low hemolysis degree (<20%) (Figure 7b). This result proves that **PAG** is safe and suitable for intravenous administration.

Drug Loading and in Vitro Release. The delivery of hydrophobic drugs to therapeutic sites is one of the major research objectives in pharmaceutical science. To evaluate the influence on the drug loading capacity of **PAG**, methotrexate (MTX) was used as the model anticancer drug. MTX was loaded into **PAG** by first incubating with codendrimer **PAG** in DMF, then dialysis against 150 mM NaCl solution to remove DMF and the free drug. The encapsulation efficiency and the drug loading content were 65% and 39%, respectively. After drug-loaded micelles were prepared, the MTX release profile from the thermosensitive **PAG** micelles was evaluated in the 150 mM NaCl solution at 37 and 42 °C (Figure 8) in separate

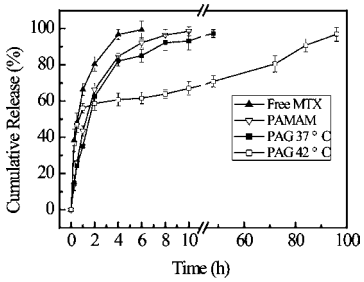

Figure 8. Cumulative MTX release in 150 mM NaCl solution at 37 and 42 °C.

trials. A control experiment using free MTX and PAMAM encapsulated MTX was also performed under similar conditions. For free MTX, complete diffusion across the dialysis membrane was found to occur within 4 h, and for PAMAM, a sustained release for 8 h was observed (both 37 and 42 °C). Release of MTX from codendrimer **PAG** was biphasic in both temperatures (37 and 42 °C), with initial burst release followed by a slow release. At 37 °C, **PAG** presented the lower release rate compared with free MTX and PAMAM; approximately 98% of the drug was released from the micelles within 48 h, which showed that the release of MTX was influenced by the architecture of codendrimer. At 42 °C, approximately 55% of MTX was released within the initial 1 h, the release rate of **PAG** was the same as free MTX. Then, approximately 10% of MTX was released during from 1 to 8 h followed by another slow release procedure (about 30%, from 8 to 96 h); the release rate decreased significantly. These results indicated that the release procedure was influenced by temperature. When the external environment temperature was above the phase transition temperature, the OEG shell of **PAG** became hydrophobic and deformed, the channels were blocked by the collapsed OEG dendron, but its scaffold was maintained; thus, the release rate of MTX became slower.[39,40] To further confirm this influence, two other temperatures (38 and 40 °C) were chosen to study the release procedure (Figure S1), which was below and above LCST of PAG separately. The results showed that the MTX release profiles from PAG at 38 and 40 °C were similar to those at 37 and 42 °C. Therefore, it proved that changes in drug release behavior were obtained from the phase transition which was induced by temperature increase. Besides, the initial burst was attributed to the drug loaded at the micellar shell, since the drug might form hydrogen bonds with the ether group of OEG dendron. Although nearly half of the encapsulated MTX may leak into blood, considering the relatively higher drug-loading capacity of 39%, PAG should be able to deliver a considerable amount of MTX to tumor and then sustain release drug at relatively higher temperature of tumor to inhibit tumor growth.

dx.doi.org/10.1021/bc300560p | *Bioconjugate Chem.* 2014, 25, 24−31

From the results obtained above, it seemed that approximately 70% MTX may be encapsulated in the outer OEG dendron shell and 30% was in the inner PAMAM core. To prove this, after the MTX-loaded PAG was prepared at 4 °C, the dialysis in 150 mM NaCl solution was performed at 45 °C to remove MTX. During this procedure, due to the temperature above the LCST, the OEG shell of **PAG** deformed and the channels were blocked; therefore, the MTX encapsulated in inner core was locked in the PAMAM core and the MTX encapsulated in outer shell was discharged, DL (9.2%) of these drug-loaded micelles was contributed by the MTX in the PAMAM core. Compared with DL (39%) before, it was considered that approximately 30% MTX was loaded in the PAMAM core. As a result, a large fraction of MTX existed in the outer shell and released at initial 4 h, a minor amount of MTX was loaded in PAMAM core, and the release procedure was influenced by temperature.

CONCLUSIONS

The codendrimer **PAG** was efficiently synthesized through the "attach to" method with excellent coverage. **PAG** formed unimers and aggregates in aqueous solutions with hydrodynamic diameter of approximately 8 and 200 nm, respectively; the CAC was found to be 0.1 mg/mL. As the thermosensitive codendrimer, **PAG** showed a sharp phase transition with small hysteresis, and the LCST was 38.2 °C. As the thermosensitive drug carrier, **PAG** showed excellent loading capacity, 39% for methotrexate (MTX). Through the different preparation method, it was proven that approximately 70% MTX was loaded into the OEG shell and 30% was encapsulated into the PAMAM core. The release studies were performed at 37 and 42 °C, which indicated that, below LCST, **PAG** presented the lower release rate compared with free MTX and PAMAM encapsulated MTX due to its core−shell structure, and above LCST, after initial 1 h, the release rate decreased significantly because the outer OEG dendron shell collapsed and the channel from core to shell was blocked but the scaffold of **PAG** was maintained. Based on the properties of high drug loading capacity and temperature-dependent drug release, this specific thermosensitive codendrimer can be used as intracellular delivery system for anticancer drugs.

ASSOCIATED CONTENT

Supporting Information

Cumulative MTX release at different temperature. This material is available free of charge via the Internet at http://pubs.acs.org.

AUTHOR INFORMATION

Corresponding Author

*E-mail: xtaowang@163.com.

Notes

The authors declare no competing financial interest.

ACKNOWLEDGMENTS

We thank Dr. Wen Li from Shanghai University for helpful discussion and suggestions and Ms. Kun Liu from the same institute for her assistance in UV/vis measurements. This work is financially supported by the National Natural Science Foundation of China (Nos. 21004079, 30772659) and the China International Science and Technology Cooperation Program for Key Projects (2008DFA31070).

REFERENCES

(1) Gupta, U., Agashe, H. B., Asthana, A., and Jain, N. K. (2006) Dendrimers: novel polymeric nanoarchitectures for solubility enhancement. *Biomacromolecules 7*, 649−658.

(2) Dhanikula, R. S., and Hildgen, P. (2005) Synthesis and evaluation of novel dendrimers with a hydrophilic interior as nanocarriers for drug delivery. *Bioconjugate Chem. 17*, 29−41.

(3) Zhang, L., Su, J., Zhang, W., Ding, M., Chen, X., and Wu, Q. (2009) Temperature-sensitive phase transition of dendritic polyethylene amphiphiles with core−shell architecture revealed by a rayleigh scattering technique. *Langmuir 26*, 5801−5807.

(4) Jelínková, M., Strohalm, J., Etrych, T., Ulbrich, K., and Říhová, B. (2003) Starlike vs. classic macromolecular prodrugs: two different antibody-targeted HPMA copolymers of doxorubicin studied in vitro and in vivo as potential anticancer drugs. *Pharm. Res. 20*, 1558−1564.

(5) Khandare, J. J., Jayant, S., Singh, A., Chandna, P., Wang, Y., Vorsa, N., and Minko, T. (2006) Dendrimer versus linear conjugate: influence of polymeric architecture on the delivery and anticancer effect of paclitaxel. *Bioconjugate Chem. 17*, 1464−1472.

(6) Greenwald, R. B. (2001) PEG drugs: an overview. *J. Controlled Release 74*, 159−171.

(7) Gajbhiye, V., Palanirajan, V. K., Tekade, R. K., and Jain, N. K. (2009) Dendrimers as therapeutic agents: a systematic review. *J. Pharm. Pharmacol. 61*, 989−1003.

(8) van Dongen, S. F. M., de Hoog, H.-P. M., Peters, R. J. R. W., Nallani, M., Nolte, R. J. M., and van Hest, J. C. M. (2009) Biohybrid polymer capsules. *Chem. Rev. 109*, 6212−6274.

(9) Astruc, D., Boisselier, E., and Ornelas, C. (2010) Dendrimers designed for functions: from physical, photophysical, and supramolecular properties to applications in sensing, catalysis, molecular electronics, photonics, and nanomedicine. *Chem. Rev. 110*, 1857−1959.

(10) Larson, N., and Ghandehari, H. (2012) Polymeric conjugates for drug delivery. *Chem. Mater. 24*, 840−853.

(11) Medina, S. H., and El-Sayed, M. E. H. (2009) Dendrimers as carriers for delivery of chemotherapeutic agents. *Chem. Rev. 109*, 3141−3157.

(12) Paleos, C. M., Tsiourvas, D., and Sideratou, Z. (2007) Molecular engineering of dendritic polymers and their application as drug and gene delivery systems. *Mol. Pharmaceutics 4*, 169−188.

(13) Jevprasesphant, R., Penny, J., Jalal, R., Attwood, D., McKeown, N. B., and D'Emanuele, A. (2003) The influence of surface modification on the cytotoxicity of PAMAM dendrimers. *Int. J. Pharm. 252*, 263−266.

(14) Roberts, J. C., Bhalgat, M. K., and Zera, R. T. (1996) Preliminary biological evaluation of polyamidoamine (PAMAM) starburst dendrimers. *J. Biomed. Mater. Res. A 30*, 53−65.

(15) Kim, Y., Klutz, A. M., and Jacobson, K. A. (2008) Systematic investigation of polyamidoamine dendrimers surface-modified with poly(ethylene glycol) for drug delivery applications: synthesis, characterization, and evaluation of cytotoxicity. *Bioconjugate Chem. 19*, 1660−1672.

(16) Kojima, C., Kono, K., Maruyama, K., and Takagishi, T. (2000) Synthesis of polyamidoamine dendrimers having poly(ethylene glycol) grafts and their ability to encapsulate anticancer drugs. *Bioconjugate Chem. 11*, 910−917.

(17) Wang, F., Bronich, T. K., Kabanov, A. V., Rauh, R. D., and Roovers, J. (2008) Synthesis and characterization of star poly(ε-caprolactone)-b-poly(ethylene glycol) and poly(l-lactide)-b-poly(ethylene glycol) copolymers: evaluation as drug delivery carriers. *Bioconjugate Chem. 19*, 1423−1429.

(18) Kojima, C., Tsumura, S., Harada, A., and Kono, K. (2009) A collagen-mimic dendrimer capable of controlled release. *J. Am. Chem. Soc. 131*, 6052−6053.

(19) Thomas, T. P., Huang, B., Choi, S. K., Silpe, J. E., Kotlyar, A., Desai, A. M., Zong, H., Gam, J., Joice, M., and Baker, J. R. (2012) Polyvalent dendrimer-methotrexate as a folate receptor-targeted cancer therapeutic. *Mol. Pharm. 9*, 2669−2676.

(20) Witte, A. B., Timmer, C. M., Gam, J. J., Choi, S. K., Banaszak Holl, M. M., Orr, B. G., Baker, J. R., and Sinniah, K. (2011) Biophysical characterization of a riboflavin-conjugated dendrimer platform for targeted drug delivery. *Biomacromolecules 13*, 507−516.
(21) Wang, H., Shao, N., Qiao, S., and Cheng, Y. (2012) Host−guest chemistry of dendrimer−cyclodextrin conjugates: selective encapsulations of guests within dendrimer or cyclodextrin cavities revealed by NOE NMR techniques. *J. Phys. Chem. B 116*, 11217−11224.
(22) Navath, R. S., Menjoge, A. R., Wang, B., Romero, R., Kannan, S., and Kannan, R. M. (2010) Amino acid-functionalized dendrimers with heterobifunctional chemoselective peripheral groups for drug delivery applications. *Biomacromolecules 11*, 1544−1563.
(23) Chung, J. E., Yokoyama, M., Yamato, M., Aoyagi, T., Sakurai, Y., and Okano, T. (1999) Thermo-responsive drug delivery from polymeric micelles constructed using block copolymers of poly(N-isopropylacrylamide) and poly(butylmethacrylate). *J. Controlled Release 62*, 115−127.
(24) Shao, P., Wang, B., Wang, Y., Li, J. and Zhang, Y. (2011) The application of thermosensitive nanocarriers in controlled drug delivery. *J. Nanomater. 2011*. DOI: http://dx.doi.org/10.1155/2011/389640.
(25) Hui, H., Xiao-dong, F., and Zhong-lin, C. (2005) Thermo- and pH-sensitive dendrimer derivatives with a shell of poly(N,N-dimethylaminoethyl methacrylate) and study of their controlled drug release behavior. *Polymer 46*, 9514−9522.
(26) Xu, J., Luo, S., Shi, W., and Liu, S. (2005) Two-stage collapse of unimolecular micelles with double thermoresponsive coronas. *Langmuir 22*, 989−997.
(27) Haba, Y., Kojima, C., Harada, A., and Kono, K. (2006) Control of temperature-sensitive properties of poly(amidoamine) dendrimers using peripheral modification with various alkylamide groups. *Macromolecules 39*, 7451−7453.
(28) Haba, Y., Harada, A., Takagishi, T., and Kono, K. (2004) Rendering poly(amidoamine) or poly(propylenimine) dendrimers temperature sensitive. *J. Am. Chem. Soc. 126*, 12760−12761.
(29) Li, X., Haba, Y., Ochi, K., Yuba, E., Harada, A., and Kono, K. (2013) PAMAM dendrimers with an oxyethylene unit-enriched surface as biocompatible temperature-sensitive dendrimers. *Bioconjugate Chem. 24*, 282−290.
(30) Li, W., Wu, D., Schlüter, A. D., and Zhang, A. (2009) Synthesis of an oligo(ethylene glycol)-based third-generation thermoresponsive dendronized polymer. *J. Polym. Sci., Polym. Chem. 47*, 6630−6640.
(31) Li, W., Zhang, A., and Schluter, A. D. (2007) Efficient synthesis of first- and second-generation, water-soluble dendronized polymers. *Macromolecules 41*, 43−49.
(32) Li, W., Zhang, A., and Schluter, A. D. (2008) Thermoresponsive dendronized polymers with tunable lower critical solution temperatures. *Chem. Commun. 0*, 5523−5525.
(33) Guo, Y., van Beek, J. D., Zhang, B., Colussi, M., Walde, P., Zhang, A., Kröger, M., Halperin, A., and Dieter Schlüter, A. (2009) Tuning polymer thickness: synthesis and scaling theory of homologous series of dendronized polymers. *J. Am. Chem. Soc. 131*, 11841−11854.
(34) Radowski, M. R., Shukla, A., von Berlepsch, H., Böttcher, C., Pickaert, G., Rehage, H., and Haag, R. (2007) Supramolecular aggregates of dendritic multishell architectures as universal nanocarriers. *Angew. Chem., Int. Ed. 46*, 1265−1269.
(35) Chen, S., Zhang, X.-Z., Cheng, S.-X., Zhuo, R.-X., and Gu, Z.-W. (2008) Functionalized amphiphilic hyperbranched polymers for targeted drug delivery. *Biomacromolecules 9*, 2578−2585.
(36) Roberts, S. K., Chilkoti, A., and Setton, L. A. (2007) Multifunctional thermally transitioning oligopeptides prepared by ring-opening metathesis polymerization. *Biomacromolecules 8*, 2618−2621.
(37) Hassouneh, W., Fischer, K., MacEwan, S. R., Branscheid, R., Fu, C. L., Liu, R., Schmidt, M., and Chilkoti, A. (2012) Unexpected multivalent display of proteins by temperature triggered self-assembly of elastin-like polypeptide block copolymers. *Biomacromolecules 13*, 1598−1605.
(38) Li, W., Li, J., Gao, J., Li, B., Xia, Y., Meng, Y., Yu, Y., Chen, H., Dai, J., Wang, H., and Guo, Y. (2011) The fine-tuning of thermosensitive and degradable polymer micelles for enhancing intracellular uptake and drug release in tumors. *Biomaterials 32*, 3832−3844.
(39) Wu, C., Wang, X., Zhao, L., Gao, Y., Ma, R., An, Y., and Shi, L. (2010) Facile strategy for synthesis of silica/polymer hybrid hollow nanoparticles with channels. *Langmuir 26*, 18503−18507.
(40) Xu, X., Flores, J. D., and McCormick, C. L. (2011) Reversible imine shell cross-linked micelles from aqueous RAFT-synthesized thermoresponsive triblock copolymers as potential nanocarriers for "pH-triggered" drug release. *Macromolecules 44*, 1327−1334.